



HAL
open science

Contribution of radar polarimetric data for the cartography in tropical environment

C Lardeux, P.-L Frison, J.-C Souyris, C Tison, Benoit Stoll, J.-P Rudant

► **To cite this version:**

C Lardeux, P.-L Frison, J.-C Souyris, C Tison, Benoit Stoll, et al.. Contribution of radar polarimetric data for the cartography in tropical environment. SPIE Asia-Pacific Remote Sensing, Nov 2008, Nouméa, New Caledonia. 10.1117/12.808091 . hal-03792257

HAL Id: hal-03792257

<https://hal.science/hal-03792257v1>

Submitted on 29 Sep 2022

HAL is a multi-disciplinary open access archive for the deposit and dissemination of scientific research documents, whether they are published or not. The documents may come from teaching and research institutions in France or abroad, or from public or private research centers.

L'archive ouverte pluridisciplinaire **HAL**, est destinée au dépôt et à la diffusion de documents scientifiques de niveau recherche, publiés ou non, émanant des établissements d'enseignement et de recherche français ou étrangers, des laboratoires publics ou privés.

Contribution of radar polarimetric data for the cartography in tropical environment

C. Lardeux^a, P.-L. Frison^a, J.-C. Souyris^b, C. Tison^b, B. Stoll^c, J.-P. Rudant^a

^aUniversité Paris-Est, laboratoire G2I/IFSA, 5 bd Descartes, 77 454 Marne la vallée Cedex 2

^b Centre National d'Etudes Spatiales, DCT/SI/AR, 18 av. E. Belin, 31 401 Toulouse Cedex 4, France

^c de Polynésie Française, B.P. 6570 98702 FAA'A Tahiti - Polynésie Française

ABSTRACT

The Support Vector Machine (SVM) algorithm is assessed for the classification of polarimetric radar data for the cartography of natural vegetation. Fully polarimetric data has been acquired in L and P bands during an AIRSAR mission over the French Polynesian Island named Tubuai. The results show significant improvement when compared to those obtained with the classification based on the maximum likelihood criterion applied to the theoretical Wishart distribution that are supposed *a priori* to be verified by radar data. Obviously, this hypothesis is not verified with the present experimental data over the study site. The addition of other polarimetric indicators to the elements of the polarimetric coherency matrix still improves the classification accuracy.

Keywords: radar, polarimetry, supervised classification, tropical vegetation, cartography.

1. INTRODUCTION

Radar data are of particular interest over tropical areas such as the French Polynesian Islands because of persistent cloudy weather. Fully polarimetric SAR data were acquired in L and P bands over the main Polynesian islands. The overall goal of this study is to assess the potential of such fully polarimetric SAR data for land-use cartography. Supervised classification algorithm of fully polarimetric data are usually based on the theoretical Wishart distribution that is *a priori* verified by radar data [1]. In order to integrate heterogeneous polarimetric descriptors (*i.e.* not only the coherence matrix used in the Wishart classification, but also other polarimetric descriptors, such the H/A/ α parameters), it is proposed to use the SVM (Support Vector Machine) classification method [2]. It is especially well suited to handle linearly non separable case by using Kernel functions. It has been mostly applied to hyperspectral remote sensed data and few studies have also been conducted with SAR data [3], [4]. The study area and radar data are presented in the second part of this paper. The third part details the SVM algorithm and describes the polarimetric indices used to define the different vectors used for the SVM algorithm. The results are discussed in the last part of the paper.

2. STUDY AREA AND DATASET

2.1 Study area

French Polynesia islands are located at the middle of the South Pacific Ocean. They are quickly evolving in the tourism industry, and from the economic and geostrategic points of view. They are thus subject to a strong environmental planning leading to landscape changes as well as to the introduction of invasive species. This study comes within the framework of the global cartography and inventory of the Polynesian landscape. We focus on data acquired over the Tubuai Island, in the Australes Archipelago at the South of French Polynesia. Tubuai is a 45 km² island with a population of about 6000 inhabitants. It is particularly relevant because of its great landscape diversity: several types of forests, agricultural fields, and residential areas. The objective is to estimate different land use class, in particular by discriminating different forest types containing four classes: *Hibiscus tiliaceus* (also called Purau), *Pinus Caribaeae* (also called Pinus), *Paraserianthes Falcataria* (also called Falcata). The 2 other classes are the one labelled "Low Vegetation", including fern lands, swamps vegetation, and few crops and the "Other" class including bare fields, low

grass fields. Several ground surveys has been carried out, and a Quickbird image acquired in August 2004 is also available to supply an accurate validation data set over the entire island.

The classes are summarized in Table 1 with the number of pixels of the radar image associated to training and control classes.

Table. 1. Classes used for the Tubuai Island classification

Type	Class	Percent cover	Training	Control
Forest	Pinus	13 %	3 000	5 000
	Falcata	7 %	2 000	2 000
	Purau	26 %	3 000	5 000
	Guava	< 1 %	500	500
Low vegetation	Fern lands	42%	2 000	2 500
	Swampy vegetation	5%	2 000	5 000
	Bare soils, roads	5 %	2 000	5 000

2.2 AIRSAR data

An AIRSAR airborne mission took place in August 2000 over the main Polynesian islands. The AIRSAR data were acquired over Tubuai along 2 passes in reverse path, in Polsar mode. The data set used in this study consists in calibrated fully polarimetric data in L ($\lambda = 23$ cm) and P ($\lambda = 67$ cm) bands with an additional C band channel ($\lambda=5.7$ cm) in VV polarization. Full polarimetric data are delivered in MLC (Multi Look Complex) format, corresponding to about 9 looks, with a resolution of 5 meters. In addition a filter has been applied over a 5x5 local neighborhood in order to reduce the speckle effects.

3. METHOD

Add a paragraph return (the "enter" key) above and below section headings and between paragraphs. Avoid headings or one-line paragraphs ("orphans") at the top or bottom of a page by using page breaks. Add additional space between paragraphs. Indentation is optional.

With SPIE *styles* paragraph spacing is automatically done for you. Section and subsection heading *styles* automatically add spaces, and orphans will always be kept together with the first paragraph under the heading. In this manner you should rarely have to force a page break to avoid an orphan.

3.1 Support Vector Machine algorithm

A brief description of SVM is made below and more details can be found in [2].

- **Linear case :**

Let us consider a two class classification problem with N training samples. Each sample is described by a Vector X_i whose components are the values observed for the different polarimetric indices investigated. The label of a sample is Y_i . For a two classes case we consider the label -1 for the first class and +1 for the other.

The SVM model ω describes the optimal hyperplane which separates the two classes (Fig. 1). The classification function f is defined as ~~$f(x) = \omega^T x$~~

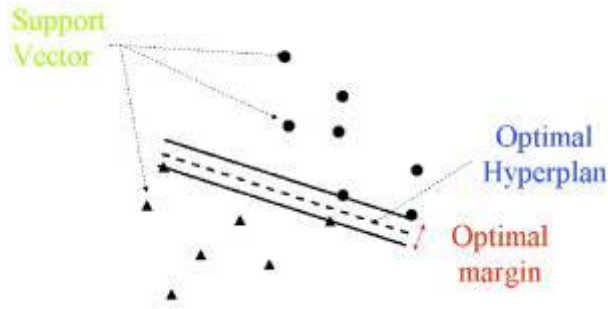


Fig. 1: SVM Classifier-Linear case

The sign of $f(x)$ gives the label of the sample. The goal of the SVM is to maximize the margin between the optimal hyperplane and the support vector. So we search for the $\min\left(\frac{\|\omega\|}{2}\right)$. It is easier in this case to use the Lagrange multiplier. The problem is then equivalent to solve:

$$\min_{\omega, b} \frac{1}{2} \|\omega\|^2 \quad \text{subject to} \quad \alpha_i \left(\omega \cdot x_i + b - 1 \right) = 0 \quad \forall i \in \{1, \dots, N_s\} \quad (1)$$

Where α_i is the Lagrange multiplier.

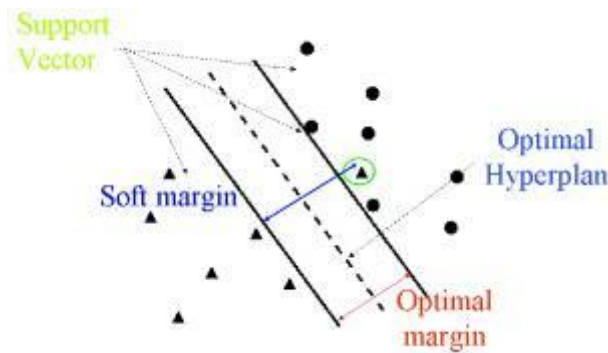


Fig. 2. SVM Classifier-Nonlinear case

Soft margin enables to get the method more robust to the noise that can be observed in the training data set.

• **Nonlinear case :**

When the classification problem is not linear (Fig. 2) the training vectors are projected into a “feature space” H of higher dimension through the feature function $\Phi : \mathcal{R}^n \rightarrow H$. In H , the data become linearly separable. Actually, it is not necessary to define the function Φ , as only the scalar product is required. This later is also called the Kernel function:

$K(x, y) = \langle \Phi(x), \Phi(y) \rangle$. The new classification function is then equal to:

$$\min_{\omega, b} \frac{1}{2} \|\omega\|^2 \quad \text{subject to} \quad \alpha_i \left(\omega \cdot \Phi(x_i) + b - 1 \right) = 0 \quad \forall i \in \{1, \dots, N_s\} \quad (2)$$

Three kernels are commonly used:

- The polynomial kernel $K(x, y) = (x \cdot y + B)^d$
- The sigmoid kernel $K(x, y) = \tanh(\gamma x \cdot y + c)$

- The RBF kernel $K(x, y) = \exp\left(-\frac{\|x - y\|^2}{2\sigma^2}\right)$

After several tests, the RBF kernel has been selected due to the best results encountered, with $\sigma = 0.5$ and a cost parameter set to 1000. A deeper analysis is performed to assess the sensitivity of the SVM method to the different parameters of the different kernels. It will be presented in future paper.

- Multiclass case :

The principle of SVM has been developed for a two class problem but it has been easily extended to a multi-class problem with several algorithms. Among them, there are: the "One Against All" (OAA) and the "One Against One" (OAO) algorithms.

If we consider a problem with K class:

The OAA algorithm consists in the construction of k hyperplane that separate respectively one class and the (k-1) other classes.

The OAO algorithm consists in the construction of $\frac{k(k-1)}{2}$ hyperplane which separate each pair of classes.

In the two cases the final label is that mainly chosen. After several tests, the OAO algorithm has been retained as well as the RBF kernel with $\sigma=0.5$ and the cost parameter equal to 1000 (soft margin).

The Libsvm library has been used [8] to implement the SVM algorithm for this study.

3.2 Polarimetric indices

To assess the suitability of the SVM method to fully polarimetric data, first a comparison is made with a maximum likelihood classifier based on the Wishart distribution that is *a priori* theoretically supposed to be verified for fully polarimetric data. In order to make a fair comparison, only the 6 elements of the polarimetric coherency matrix are taken into account. This latter is constructed from the scattering vector k_p expressed in the Pauli basis as follows:

$$k_p = \frac{1}{\sqrt{2}} \begin{pmatrix} S_{HH} + S_{VV} \\ S_{HH} - S_{VV} \\ 2.S_{HV} \end{pmatrix}, [T] = k_p . k_p^{*T} \quad (3)$$

S_{wx} denotes the scattering matrix element corresponding to the w/x polarization for the receiving/transmitting wave (w, x referring to horizontal, H, or vertical, V, linear polarization)

Consequently a 9 components vector is defined, called V_{wish} , that is constituted of 9 real elements: the 3 diagonal ones, with the addition of the real and imaginary part of the 3 off diagonal elements. When the 3 bands are combined a $2 * 9 + 1 = 19$ components vector is used, corresponding to the combination of V_{wish} for the L and the P band with the addition of the intensity in VV polarization of the C band.

On the other hand, to assess the contribution of the concerned different polarimetric indices, another vector, called V_{Full} is defined and constituted of 54 elements. These are detailed hereafter, and are summarized Table 2:

- The intensities in the 2 co- and 1 cross- polarized channel in linear and circular polarization:

$$I_{wx} = |S_{wx}|^2 \quad (4)$$

where w and x refer to H, V, left, L, and/or right, R, circular polarization.

- The Span:

$$SPAN = I_{HH} + 2 I_{HV} + I_{VV} \quad (5)$$

Local heterogeneities are taken into account through the coefficient of variation $c_v = \frac{\sigma}{\mu}$, σ and μ are representing the standard deviation and mean of the intensities in the linear and circular polarization computed over a local neighbourhood.

- The ratio between the following intensities:

$$\frac{I_{HV} I_{VH} I_{HH} I_{LL}}{I_{HH} I_{VV} I_{LL} I_{RR}} \quad (6)$$

- The modulus of the degree of coherence, $\rho_{HH-VV}, \rho_{HV-HH}, \rho_{HV-VV}, \rho_{LL-LR}, \rho_{RR-LR}, \rho_{LL-RR}$ computed as follow:

$$|\rho_{w,x,y,z}| = \frac{|\langle S_w S_x^* S_y^* S_z^* \rangle|}{\sqrt{\langle |S_w|^2 \rangle \langle |S_x|^2 \rangle \langle |S_y|^2 \rangle \langle |S_z|^2 \rangle}} \quad (7)$$

where w, x, y, z, stands for H, V, L and R polarization

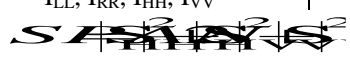
- The minimum and maximum power of the backscattered wave, I_{min} and I_{max} resp, for all the polarization configuration of the emitted wave. In fact, due to the high correlation observed between S and I_{max} , the latter is not retained, and is replaced by the ratio I_{min} / I_{max}
- The minimum of the degree of polarization of the received wave $d_{P_{min}}$ for all the polarization configurations of the emitted wave. The degree of polarization is defined as

$$d_{-P} = \frac{\sqrt{S_2^2 + S_3^2 + S_4^2}}{S_1} \quad (8)$$

S_1, S_2, S_3, S_4 being the 4 elements of the Stokes vector.

- The 3 parameters $H/A/\alpha$ representing the entropy, the scattering mechanism, and the anisotropy [5]
- The 3 intensity parameters of the Freeman decomposition [6], $P_s, P_d,$ and P_v corresponding to the weight of the single, double, and volume in the backscattered response.
- The 5 Euler parameters $m, \gamma, \nu, \tau,$ and ψ Details about their calculation from the Stokes parameters are given in [7].

Table. 2. Vectors configuration used in the SVM classification

V_{Wish}		V_{Full}
T elements		T elements
		$I_{LL}, I_{RR}, I_{HH}, I_{VV}$  $c_{v-HH}, c_{v-HV}, c_{v-VV},$ $c_{v-LL}, c_{v-RR}, c_{v-LR},$ $I_{HV}/I_{HH}, I_{HV}/I_{VV}, I_{HH}/I_{VV}$ $I_{RR}/I_{LR}, I_{LL}/I_{LR}, I_{LL}/I_{RR}$ $\rho_{HH-VV}, \rho_{HV-VV}, \rho_{HV-HH}$ $\rho_{LL-LR}, \rho_{RR-LR}, \rho_{LL-RR}$ $I_{min}, I_{max} / I_{min},$ $d_{P_{min}}, d_{P_{max}}, \Delta(d_{-P})$ Euler parameters: $m, \gamma, \psi, \nu, \tau$ $H/A/\alpha$ Freeman parameters: P_s, P_d, P_v
# elements	9	54

All the polarimetric indices have been estimated on a 5x5 local neighborhood on the data that has been previously filtered [8].

3.3 Greedy analyses

To estimate the contribution of the different polarimetric indices, a greedy backward method is developed. It is an iterative procedure that begins with the classification obtained with the initial 54 components V_{Full} vector. Then, the SVM classifications involving the 54 vectors that can be derived from all the combination of 53 polarimetric indices chosen among the 54 original ones are made. The 53 elements vector retained is that corresponding to the higher classification accuracy. This procedure is repeated until the remaining only 3 polarimetric indices.

On the other hand, to evaluate the polarimetric index that improve the most the classification results obtained with a given vector V_{ref} , a greedy forward approach is made as follow: the classifications are made with all the vectors that are obtained from V_{ref} with the addition of one of each of the polarimetric indices that are tested. The vector retained is the one corresponding to the highest classification accuracy.

4. METHOD

4.1 Comparison between Wishart and SVM classifications

In order to evaluate the potential of the SVM method, a comparison is first conducted with a supervised Wishart classifier based on the *a priori* knowledge of the statistical properties of the coherency matrix elements [1]. In order to conduct a fair comparison between SVM and Wishart classifier, the SVM classification considers here a vector, denoted V_{WISH} , including only the nine elements of the coherency matrix (i.e. the 3 real diagonal elements and the real and imaginary parts of the 3 off-diagonal elements). In addition, the comparison has also been made when the L, P, and C bands are combined together. In that case, the vector used for the SVM algorithm, denoted V_{WISH_PLC} , includes 19 elements: i. e. the 2 x 9 elements of the coherency matrix of L and P bands, with the addition of the intensity I_v acquired at C band. The results are given Table 3. The classification accuracy is given by the Mean Producer Accuracy (MPA) which consists in the average of the diagonal terms (expressed in %) of the confusion matrix. It allows to better take into account the detection of each individual class when their populations are different as in the present case (see for example the Guava with respect to Pinus population Tab. 1).

Table 3: Mean Producer accuracy (%) of the Wishart and the SVM classifications

Type	Class	L Band		P band		L + P +C bands	
		Wishart	SVM	Wishart	SVM	Wishart	SVM
Forest	Pinus	32	74	56	71	81	99
	Falcata	69	80	37	64	75	99
	Purau	48	78	61	85	75	98
	Guava	76	88	66	74	74	100
Low vegetation	Fernland	62	93	49	88	56	98
	Swampy vegetation	85	97	92	93	95	99
	Bare soil	90	98	91	96	91	99

On the whole, the SVM algorithm gives much better results than those obtained with the Wishart classifier, with MPA values of 87% and 82% for L and P bands, which is about 20% higher than the Wishart classifier results. The poor performance of the Wishart classifier tends to show that there is a discrepancy between the supposed Wishart distribution and the one observed in the experimental data. We are obviously in a situation where the stationary assumptions are not

met. On the contrary, the SVM algorithm does not take into account any *a priori* information about the statistical distribution of the processed data. The good accuracy obtained indicates the potential of the non linear kernel theory for classification, for training dataset which has to be the most representative of each class. It can be noted the remarkable accuracy (MPA=99%) obtained with the SVM method when the P, L, and C bands are combined. The 99 % MPA value observed, remarkably high, is not representative of the reality, since a lot of approximations are made, such as reducing the numerous different landscapes to only 7 pure classes. However, the relative differences between the classification accuracies are significant, since all are based on the same training and control classes.

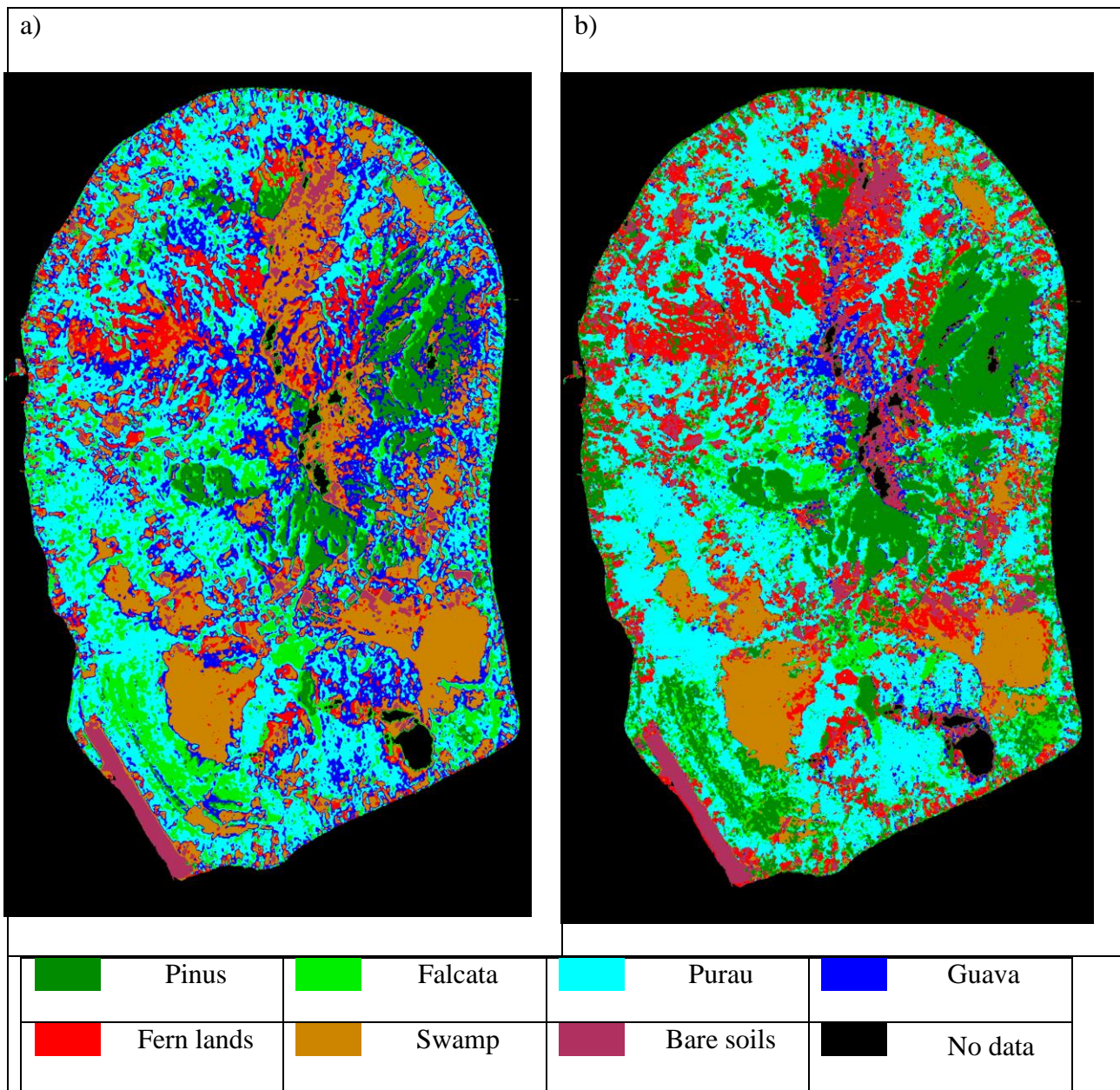


Figure 3: Images of the classification obtained when P, L, and C bands are combined: a) Wishart classifier (MPA = 78%) and b) SVM for the 19 indicators of the *V_WISH_PLC* vector (MPA=99%).

On the other hand, the MPA values are about 5% higher for L band than for P band whatever the classification method used. The analysis of different confusion matrices shows, as it can be expected, that there is a higher confusion at P band between the Fernland and swampy vegetation classes, *i.e.* the P band is less sensitive to low vegetation densities. However, it is more difficult to give an interpretation about the behaviour observed over forest classes. Despite better penetration capabilities in forest canopies at low frequencies, at the exception of Purau, a higher confusion between forest species is observed at P band than at L band.

The images corresponding to the classification obtained with Wishart and SVM classifiers when the P, L, and C bands are combined are shown in Figure 3. It is particularly obvious that the large number of pixels that are wrongly classified as Guava with the Wishart classification are significantly reduced with the SVM classification.

These results indicate that although the SVM method is not especially developed for radar data, it presents nevertheless a significant potential for radar polarimetric data classification.

4.2 Polarimetric indices contribution

This section analyses the contribution of the different polarimetric indicators listed in Table 2 according to the greedy forward or backward methods applied to the SVM algorithm.

When only one single frequency polarimetric band is considered (*i.e.* L or P band) the 54 polarimetric indicators (listed in Table 2) define a 54 components reference vector noted V_{FULL} . Figure 4 shows the classification overall accuracy (MPA) with respect to the number of primitives. It is the result of the different steps of the greedy backward algorithm from the V_{FULL} initial vector, at L and P bands. Both L and P bands indicate a similar behaviour: a large plateau around the MPA maximum value is reached for a number of primitives ranging approximately between 20 and 45. The MPA maximum value is 91% and 88% for L and P band respectively, representing a gain of 4% and 6% by comparison with the results obtained with the V_{WISH} vector. Below 10 primitives, the classification performance shows a dramatic decrease (down to 63% and 67% for L and P band) due to too reduced remnant information. It is also worth noting that a marked decrease (6% and 9% for L and P bands) is also observed for a primitive number higher than 48 for both bands, indicating that some polarimetric indicators introduce high confusion for classification. An analysis of the concerned polarimetric indices shows that 7 particular indicators are among the less discriminative both for L and P band: 4 of the Euler parameters ν , ψ , γ , and τ and the 3 phases of the degrees of coherence ϕ_{ll-rr} , ϕ_{rr-lr} , and ϕ_{hh-hv} . It is not surprising as the Euler parameter are especially defined to account for the characterization of deterministic target inducing fully polarized radar response, which is not the case over vegetated surfaces. The non efficiency of the phases of the degrees of coherence is also expected over these dense vegetated areas, although useful information can be extracted from some of these parameters over others types of surface, such as urban or spared vegetation areas for example [9], [10]. On the other hand, polarimetric indicators occupying the left part of the curve are not necessarily the most significantly discriminating ones. This is due to the constant performance of the classification on the plateau region which indicates that each individual indicator has a negligible contribution. Consequently, in that horizontal part of the curve, the greedy backward method can remove indicators with more intrinsic discriminating behaviour than others (see for example, the entropy H with regard to ϕ_{vv-hv} at P band).

Moreover, it has to be pointed out that the greedy algorithms are depending on the original subset of primitives (defining the initial vector) as well as the subset that is investigated to add or remove the indicator at the next iteration. For example, a forward approach with the initial vector defined by the first 5 primitives would give a different ranking. Several tests (not shown here) have illustrated this behaviour, however, the resulting curves are similar to those presented in fig. 5, confirming that a different combination of indicators can give similar performance. In particular, a greedy forward analysis based on V_{WISH} initial vector shows that the addition of different coefficients of variation, intensity channels (or ratio, or Freeman parameters), as well as the entropy, allows to obtain the same maximum classification accuracy.

These results show that even if good classification results are obtained when only the elements of the coherency matrix are considered, the addition of other polarimetric indicators contributes to a systematic improvement of the classification accuracy of 5% and 7% for L and P bands. Furthermore, the greedy backward method allows to point out some confusing indicators leading to a reduction of the classification results (the Euler parameters ν , ψ , γ , and τ , and the 3 phases of the degrees of coherence ϕ_{ll-rr} , ϕ_{rr-lr} , and ϕ_{hh-hv}) although, as already mentioned, it does not allow a deeper comparison between the different indicators.

Concerning the contribution of the combination of P, L, and C bands, the MPA value obtained when all the 110 parameters are combined (*i.e.* 2 x 54 at L and P bands with the addition of I_{vv} and c_{v-vv} at C band) is 57%, indicating the high degree of confusion introduced here again by different polarimetric indicators. A similar greedy backward analysis from these 110 existing primitives cannot be considered due to computational time constraint. As an illustration, about

53 hours are needed on a Pentium4 630 - 3.0 GHz processor to remove one among one hundred primitives. Consequently, the results shown in Figure 4 are based on the initial 19 components vector V_{WISH_PLC} , the right and left parts of the curve resulting from a greedy forward and backward analysis respectively. The addition of other polarimetric indicators to V_{WISH_PLC} does not improve the classification results, which observe a constant MPA value of 99% (as far as the 54 indicators shown here are considered). Details about these different indicators (which are mostly intensity parameters) are not given as the plateau observed here again hampers to evaluate more deeply their discriminating contribution.

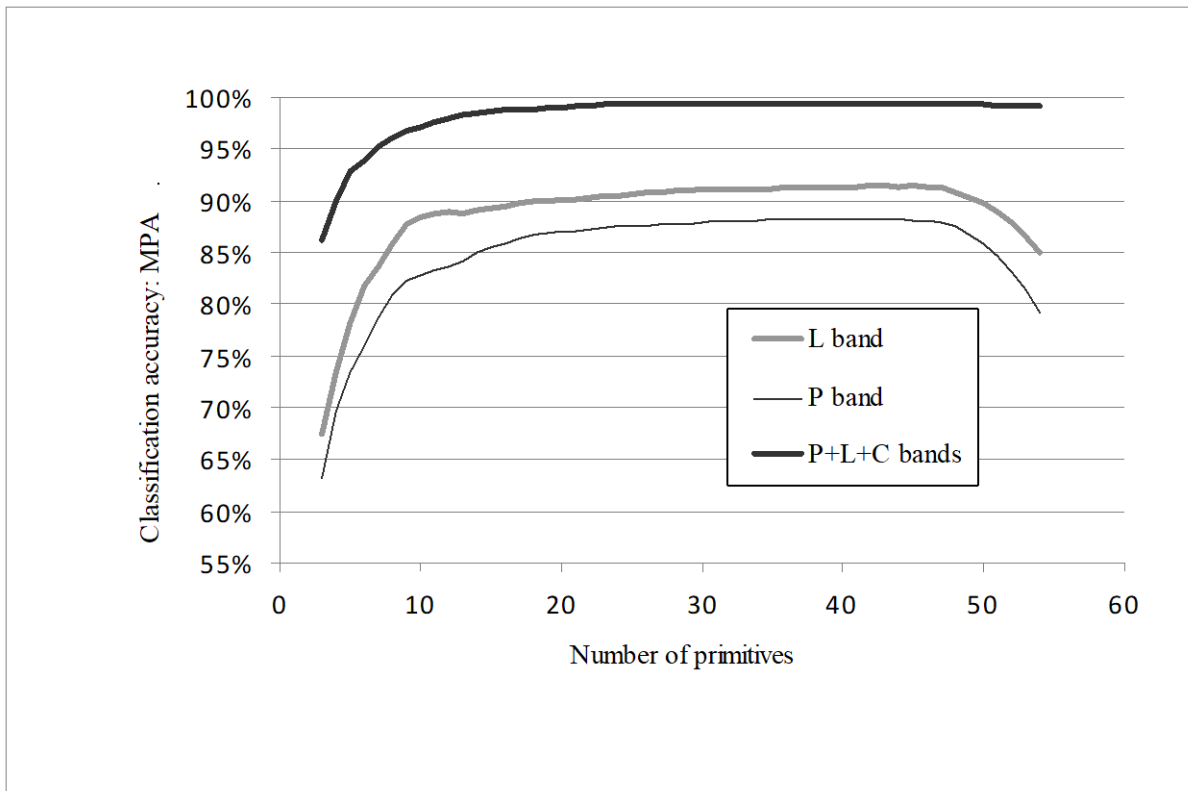


Fig. 4: Contribution of the polarimetric indicators (or primitives) for L band, P band, and when P, L and C bands are combined together.

5. CONCLUSION

This study addresses the potential of the SVM algorithm for the classification of polarimetric SAR data. The SVM algorithm is especially suited to account for numerous and heterogeneous parameters, which enables to take into account a large bunch of polarimetric indicators. The proposed method has been applied to data that have been acquired over a French Polynesian Island during an AIRSAR mission. When only the elements of the coherency matrix are involved, the SVM algorithm gives a good overall accuracy with MPA values of 87% for L band, 82% for P band, and 99% when L, P and C bands are combined. It represents a high improvement of about 20% by comparison with the Wishart classification. These results indicate that the theoretical Wishart distribution is obviously not observed by the experimental data, while, by contrast, no *a priori* information is required for the SVM algorithm. The addition of polarimetric indicators allows to improve of about 5% the results (MPA = 91%, 88%, for L, P bands respectively) with respect to those involving the coherency matrix elements. As a consequence, a recommendation for optimal use would be to consider only the elements of the coherency matrix for the SVM classification, which shows a good compromise between

the number of involved polarimetric indices and the classification accuracy obtained. The greedy analysis performed allowed to clearly point out polarimetric indicators introducing significant confusion in the classification at both L and P bands. These are the Euler parameters and 3 differential phases of the degree of coherence, which is not surprising over such dense vegetative area. However, the greedy algorithm does not allow drawing conclusion about the most discriminating parameters. Nevertheless, these results demonstrate the high potential of the SVM algorithm for radar polarimetric data supervised classification. Additional analyses have to be performed in the future, in particular to assess more precisely the influence of the kernel used in the SVM method.

6. REFERENCES

- [1] Lee J. S., Grunes M. R., Kwok R., "Classification of multi-look polarimetric SAR imagery based on complex Wishart distribution", *Int. Journal Remote Sensing*, vol. 15, n° 11, pp 2299-2311, 1994.
- [2] Burges C. J., "A tutorial on Support Vector Machines for pattern recognition", *Data Mining Knowledge Discovery*, U. Fayyad, Ed. Kluwer Academic, 1998.
- [3] Mercier G. and Girard-Arduin F., "Unsupervised Oil Slick Detection by SAR Imagery using Kernel Expansion", *Int. Geosci. Remote Sensing Symp.*, vol. 1 pp 494-497, July 2005.
- [4] Tison C., Pourthié N., Souyris J.-C., "Target recognition in SAR images with Support Vector Machine (SVM)", *IGARRS'07, Barcelona (Spain)*, July 2007.
- [5] Cloude S. R. and Pottier E., "An entropy based classification scheme for land applications of polarimetric SAR", *IEEE Trans. Geosci. Remote Sensing*, vol. 35, n°1, pp 68-78, 1997.
- [6] Freeman A., Durden S. L., "A three component scattering model for polarimetric SAR data", *IEEE Trans. Geosci. Remote Sensing*, vol. 36, n° 3, pp 963-973, 1998.
- [7] Huynen J. R., "Phenomenological theory of radar targets", *Doctoral thesis, Delft University, the Netherlands*, 1970.
- [8] Lee J.-S., Grunes M. R., de Grandi G., "Polarimetric SAR speckle filtering and its implication for classification", *IEEE Trans. Geosci. Remote Sensing*, vol. 37, n° 5, pp 2363-2373, 1999.
- [9] Lee J. S., Schuler D. L., Ainsworth T. L., "Polarimetric SAR data compensation for terrain azimuth slope variation", *IEEE Trans. Geosci. Remote Sensing*, vol. 38, n° 5, pp 2153-2163, 2000.
- [10] Moriyama T., Uratsuka S., Umehara T., Satake M., Nadai A., Maeno H., Nakamura K., Yamaguchi Y., "A study on extraction of urban areas from polarimetric synthetic aperture radar image", *IGARSS'04*, pp. 703-706, Anchorage, AL, September 2004.